electronics

MDPI

Article

Electromagnetic Loss Analysis of a Linear Motor System Designed for a Free-Piston Engine Generator

Yunqin Hu [1,*], Zhaoping Xu [2], Lijie Yang [2] and Liang Liu [2]

[1] Department of Communication Engineering, Nanjing University of Posts and Telecommunications, Nanjing 210003, China

[2] School of Mechanical Engineering, Nanjing University of Science and Technology, Nanjing 210094, China; xuzhaoping@njust.edu.cn (Z.X.); yangljname@foxmail.com (L.Y.); l.liu@njust.edu.cn (L.L.)

* Correspondence: huyq@njupt.edu.cn

Received: 8 March 2020; Accepted: 4 April 2020; Published: 8 April 2020

Abstract: A free-piston engine generator is a new type of power generating device, which has the advantages of high efficiency and simple structure. In this paper, a linear motor system composed of a moving-coil linear motor with axial magnetized magnets and a H-bridge pulse-width modulation (PWM) rectifier is designed for portable free-piston engine generators. Based on the finite-element model of the motor and physical model of the rectifier, the combined electromagnetic model is presented and then validated by the prototype-tested results. The electromagnetic processes of the linear motor system are simulated. The electromagnetic losses during the standard working cycle are analyzed. Under the rated reciprocating frequency of 50 Hz and the rated reciprocating stroke of 36 mm, the mechanical-to-electrical energy conversion efficiency of 86.3% can be obtained by the linear motor system, which meets the requirement of portable free-piston engine generators.

Keywords: electromagnetic analysis; electromagnetic loss; modeling and validation; moving-coil linear motor; PWM rectifier; free-piston engine generator

1. Introduction

A free-piston engine generator (FPEG) is a novel power generating device, which is a combination of a free-piston engine and a linear motor [1]. This new type of power generating device has attracted more and more scholars' attention due to its potential advantages of high efficiency, simple structure and renewable alternative fuels adaptability [2]. The device can be used in portable power generation, electric vehicles and communication base stations [3].

The structure of a portable FPEG, studied in this paper, is shown in Figure 1. The device consists of a mechanical body, a rectifier for power conversion, a battery for energy storage and a controller. The mechanical body includes a free-piston engine, an air-spring for kickback, and a linear motor. Compared with the traditional engine generator, the crankshaft is canceled, and the free-piston is directly connected to the mover of a linear motor. The piston-mover assembly is the only moving part of the device [4]. This structure has the advantages of compact, low mass, easy manufacture, and low maintenance cost.

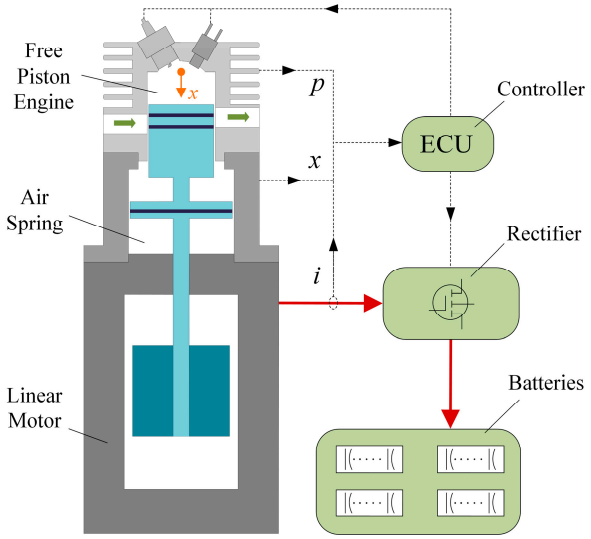

Figure 1. Free-piston engine generator sketch.

As the free-piston is not limited by the crankshaft, the reciprocating motion of the piston-mover assembly completely depends on the instantaneous forces acted on it. The forces include combustion pressure, electromagnetic force and spring force. The compression ratio of a FPEG is variable, thus multiple renewable alternative fuels can be used by the device without any structural changes. These features make the development of a FPEG competitive and valuable.

A working cycle of the portable FPEG, studied in this paper, is shown in Figure 2. A working cycle has two strokes: compression stroke and expansion stroke. In the compression stroke, the piston-mover assembly moves up from the bottom turning center (BTC) to the top turning center (TTC), and the mixture of air and fuel in the combustion chamber is compressed. In the expansion stroke, the compressed mixture of air and fuel is burned and releases heat instantly, so the piston-mover assembly moves down from the TTC to BTC driving by the combustion pressure.

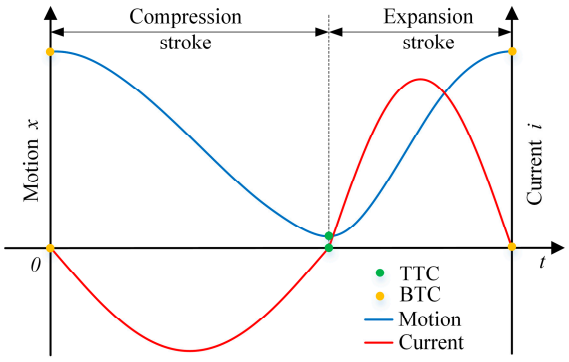

Figure 2. Working cycle of the free-piston engine generator.

During the stable running, the linear motor works in generating mode all the time. The electromotive force (EMF) in the coil of the motor is quasi-sine wave, and the generating current in the coil is controlled as standard sine wave by the rectifier, and the electrical energy will be stored in the battery in the form of direct current. During the starting of the device, the linear motor must work briefly in motoring mode to start the motion of the piston-mover assembly.

The linear motor and the rectifier make up the linear motor system of the FPEG. Its performance affects the energy utilization efficiency of the FPEG. Many researchers have been working on the design of the linear motor for an FPEG [5–7]. Wang [8] proposed and designed a three-phase moving-magnet

linear motor for the application of an FPEG. Its electromagnetic characteristics were predicted by analytical expressions and verified by finite element methods.

Xu [9] proposed a single-phase moving-coil linear motor with radial magnetized magnets for the application of an FPEG, its analytical model was created, and its thrust force and the coil inductance were investigated. This kind of single-phase moving coil linear motor has the advantage of less moving mass, faster response and better controllability, but the generating efficiency is not high enough as there is a high eddy loss in the radial magnetized magnets.

Chen [10] proposed a single-phase, short-stroke and large thrust axial magnetized linear motor. A combined electromagnetic model composed of a finite element model and mathematical model of the controller was built, and the simulated results were compared with the tested results. This kind of single-phase axial magnetized linear motor was reported to have higher efficiency than radial magnetized. In this research, the electromagnetic loss in the power converter was not considered.

Zheng [11] proposed a 1 kW moving-magnet linear motor for the FPEG application. The power densities, thrust fluctuation, and thermal field of the linear motor were investigated, but the electromagnetic efficiency of the linear motor was not reported in the paper. Xu [12] designed a similar 3 kW linear motor with I-shaped and rectangular designs for the same application. The theoretical efficiency of 90% to 95% was reported under the reciprocating moving speed of 3 to 5 m/s.

In reference [13], a single-phase moving-magnet linear motor was proposed for an FPEG. The three-dimensional finite element model was established, and its boundary conditions were presented and explained in detail. By using the model, an electromagnetic analysis was carried out. The performance of the linear motor under reciprocating frequency 75 Hz was investigated and analyzed. The electromagnetic efficiency of 82% was obtained by the linear motor.

As per the literature review above, some informative works about the linear motor designed for a FPEG have been reported. Analytical and finite element models have been created to analyze the efficiency of the linear motor, but few works try to research the linear motor and its power driving system as a whole system. The authors believe that a combined electromagnetic loss analysis is an efficient path to assess and optimize the total efficiency of a linear motor system [14,15].

In order to meet the requirements of a portable FPEG, this paper will present a novel linear motor system, which is considered to have the advantages of low moving mass, fast response, easy controllability and high efficiency. Based on the finite-element model of the motor and physical model of its power driving system, a combined electromagnetic model is presented and validated by the prototype. Then the electromagnetic loss of the motor system is analyzed in detail.

2. System Design

2.1. Linear Motor Design

The linear motor system is the most important component of the FPEG. It must meet some special requirements of the FPEG, such as low moving mass, fast response, easy controllability and high energy conversion efficiency [16,17]. A single-phase moving-coil linear motor with embedded axial magnetized magnets is designed in this paper. As shown in Figure 3, the motor can be divided into three parts: the stator, the mover and the shell. The stator is made up of an inner stator and an outer stator, each stator includes an axial magnetized magnet and two iron cores, and the magnet is located between the two iron cores. The magnetization direction of magnet in the inner and outer stators is opposite. The mover is made up of two reverse series moving-coils and a high strength plastic support. The mover is located in the air gap between the inner and outer stators.

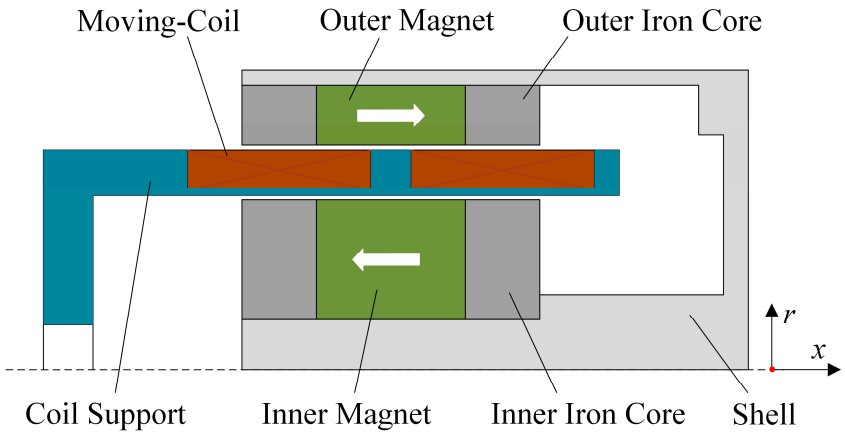

Figure 3. Sketch of the designed linear motor.

Table 1 lists the main parameters of the linear motor in detail. Additionally, the neodymium iron boron "N42SH" is a choice for the magnet material to achieve higher residual magnetic flux density, temperature stability and coercive force. The electrical pure iron "DT4" is a choice for the core material. Compared with silicon steel sheets and low carbon steel, the electrical pure iron is more suitable for this kind of moving-coil linear motor. It has lower manufacturing costs and better permeability performance. A kind of aluminum alloy is a choice for the shell material for low density and low magnetic permeability. A kind of high strength plastic "PTFE" is a choice for the coil support material. It has the advantages of non-magnetic, non-conductive and high strength.

Table 1. Parameters of the designed linear motor.

Items	Value
Diameter of outer stator	114 mm
Thickness of outer stator	12 mm
Diameter of inner stator	68 mm
Thickness of inner stator	24 mm
Length of core	15 mm
Length of PM	30 mm
Length of coil area	37 mm
Width of air gap	10 mm
Turns of two coils	128
Max stroke	40 mm

2.2. Rectifier Design

The rectifier used in the FPEG not only must have high efficiency, but also must have two additional functions. The first function is that the rectifier must be controllable for adjusting the generating current of the motor. The second function is that the rectifier must be used as an inverter during the starting process of the FPEG to start the motion of the piston-mover assembly.

This is because the reciprocating motion of the piston-mover assembly in a FPEG completely depends on the instantaneous forces acted on it. Between the forces of combustion pressure, electromagnetic force and spring force, the electromagnetic force is the only one which can be controlled to adjust the piston motion. The control of electromagnetic force of the motor is to control the coil current of the motor according to every stroke, so the rectifier must be controllable.

An H-bridge pulse-width modulation (PWM) rectifier is designed to meet the requirements of the FPEG. As shown in Figure 4, this is a voltage source PWM rectifier. During the stable running of the FPEG, the linear motor works in generating mode all the time, and the rectifier works in rectify and boot mode. The electromotive force (EMF) in the coil of the motor is quasi-sine ware. When the EMF of the motor is positive, K3 will be controlled by PWM signals and the others remain off, and its

current path of PWM on and PWM off is presented in Figure 4. When the EMF is negative, K1 will be controlled by PWM signals and the others remain off.

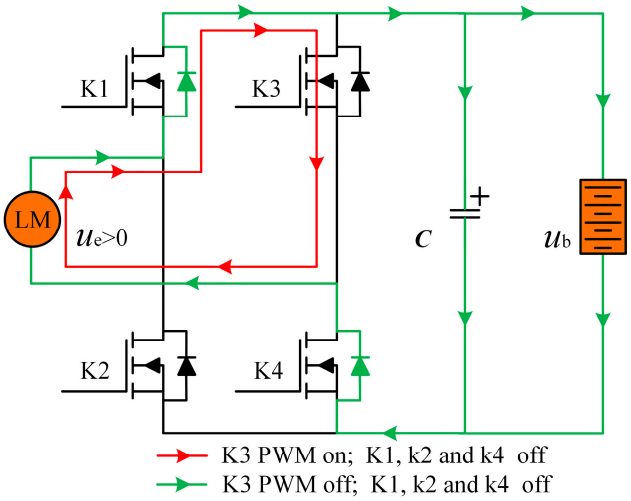

Figure 4. Designed rectifier and its typical current path.

During the starting process of the FPEG, the linear motor can briefly work in motoring mode. At this point, the PWM rectifier works as a PWM inverter. When the linear motor needs to be motoring from bottom to up, K1 keeps on, K4 will be controlled by PWM signals, and the others remain off. When the linear motor needs to be motoring from up to bottom, K3 keeps on, K2 will be controlled by PWM signals, and the others remain off. We call this type of control the limited unipolar control method. This control method can reduce the electromagnetic loss as much as possible.

Table 2 lists the main parameters of the designed PWM rectifier in detail, including the control parameters and electromagnetic parameters of the power switch devices. As shown in the table, metal oxide semiconductor field effect transistors (MOSFET) are a choice for the power switch to reduce the electromagnetic loss. The parameters will be used by the model in the next section.

Table 2. Parameters of the designed pulse-width modulation (PWM) rectifier.

Items	Value
Rated voltage of the battery	120 V
Capacitance of filter capacitor	400 μF
Max Current of K1~K4	70 A
On-resistance of K1~K4	25.5 mΩ
Turn-on time of K1~K4	24 ns
Rise time of K1~K4	16 ns
Turn-off time of K1~K4	62 ns
Fall time of K1~K4	45 ns
Diode forward voltage of K1~K4	1.3 V
PWM Frequency of K1~K4	40 kHz

3. Modeling and Validation

3.1. Linear Motor Model

The electromagnetic model of linear motors can be divided into an analytical model and finite element model. Compared to the analytical model, the finite element model has the advantages of being easy to model and quick to calculate. Additionally, the finite element model can consider the end effect and take magnetic flux leakage into account and calculate more accurately. In this paper, a transient finite element method with a motion solver is used to model the linear motor designed for the FPEG.

The model of the linear motor is shown in Figure 5. This model is a two-dimensional transient finite element model with a motion region. At this point, the mover is in the middle of the stroke, and the position is defined as the original point of the mover, as shown in Figure 5. The magnetic field is mainly distributed in ferromagnetic materials, and the leakage flux is relatively small. In order to display the internal structure, the meshes in the air box of the calculation region are hidden.

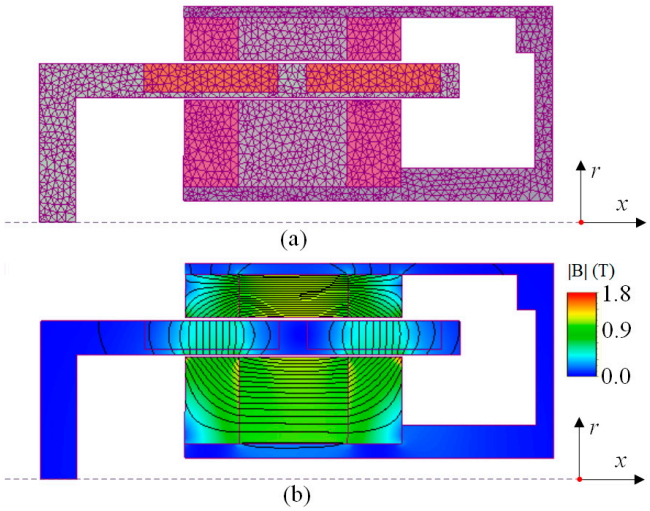

Figure 5. Finite element model of the linear motor, (**a**) mesh, (**b**) flux density.

3.2. Combined Simulation Model

In order to analyze the electromagnetic loss of the designed PWM rectifier, its physical model is established by using the power electronics toolbox in the software of MATLAB. Supported by the finite element software we used to create the model of the linear motor, the finite element model of the linear motor is embedded into the MATLAB software. The MATLAB software calls the finite element software in every time steps, so the real combined simulation can be realized.

As shown in Figure 6, the combined model consists of four parts: linear motor finite element model, rectifier model, rectifier controller, and free-piston engine model. The rectifier controller provides PWM signals to the four power switch devices of the rectifier model. The PWM signals are calculated based on the current feedback of the motor, and a discrete proportional integral differential (PID) algorithm is used in this paper. The free-piston engine model is created according to the difference equations described in [16]. The free-piston engine model is used to output the piston motion trajectory to drive the linear motor finite element model.

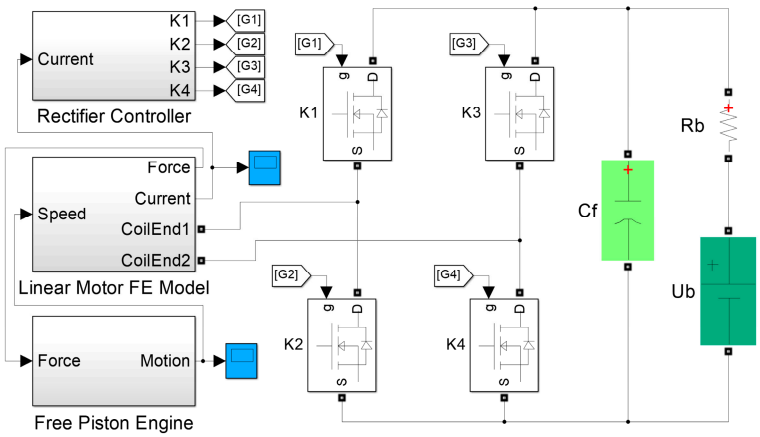

Figure 6. Combined model of the linear motor system.

3.3. Model Validation

A prototype of the linear motor system designed in the last section is developed. Figure 7 shows the prototype and its test platform. The test platform consists of five parts: the developed linear motor, prototype, the developed PWM rectifier, an air spring, a free piston engine and a battery.

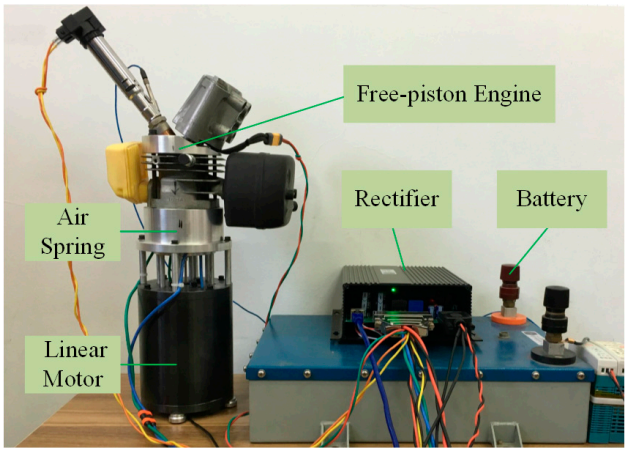

Figure 7. Prototype of the linear motor system and its test platform.

The piston bore of the engine is 48 mm with the max stroke of 38 mm and the effective compression ratio of 7.8. It uses gasoline direct injection and spark ignition combustion under the excess air ratio of 1.1. The indicated power of the engine is about 1.5 kW, and the indicated thermal efficiency is 37% [17]. The piston bore of the air spring is 65 mm, which is bigger than the piston bore of the engine. The moving mass of both the piston and cylinder is about 0.5 kg.

A displacement sensor is connected to the mover of the linear motor, and a current sensor is installed in the alternating current side of the rectifier, so the real-time piston-mover position and the coil current of the linear motor can be tested. Based on the test platform, the combined model created in the last section is validated by comparing the simulated results with the prototype tested results.

Figure 8 shows the simulated and tested movement of the piston-mover assembly. As shown in the figure, a simplified testing cycle is used. The stroke of the testing cycle is 14 mm, and the reciprocating frequency is about 23 Hz. The testing cycle has two processes. In the first process, the linear motor works in motoring mode, the PWM rectifier works as an PWM inverter to drive the linear motor move from top to bottom, and the gas spring brakes the motion. In the second process, the gas spring drives the linear motor move from bottom to top, the PWM rectifier works in rectify and boost mode, and the linear motor works in generating mode to brake the motion.

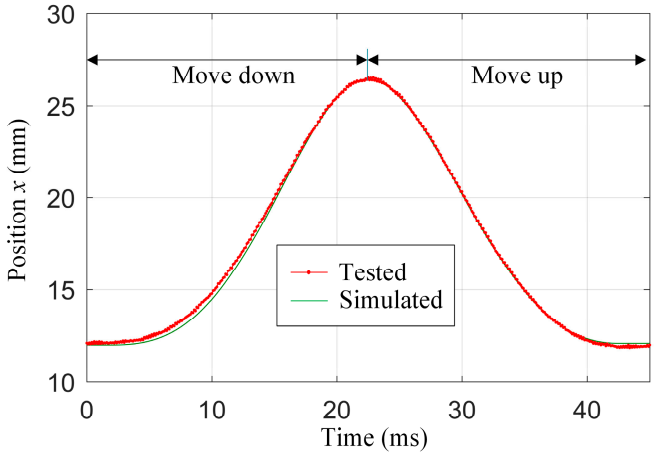

Figure 8. Comparison of tested and simulated movement.

Figure 9 shows the simulated and tested coil current of the linear motor during the testing cycle. In each stroke, the coil current is controlled to standard sine wave by the PWM rectifier. The root mean square (RMS) currents in the two processes are 16.8 A and 9.8 A. The difference between the two RMS currents is due to the losses during the reciprocating motion cycle, including the electromagnetic loss discussed in the paper and the mechanical loss.

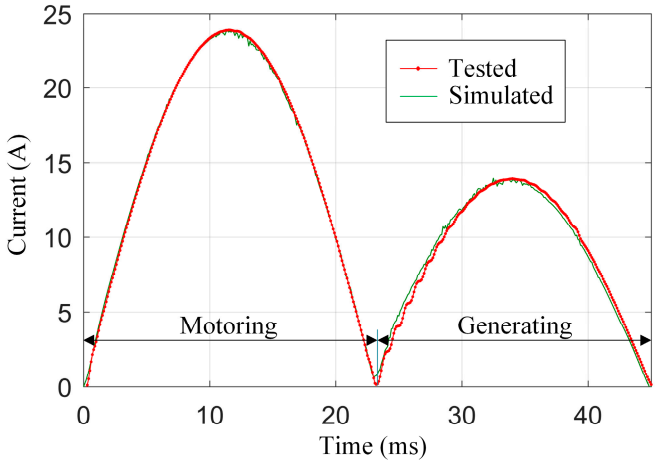

Figure 9. Comparison of tested and simulated current.

Figure 10 shows the simulated and tested PWM ratio of the PWM rectifier during the testing cycle. As shown in the figure, the results are consistent, especially when the linear motor system is operating in the power generation state. This consistency validates the combined model created in the last section, and indicates that the most electromagnetic loss of the linear motor system has been modeled by the combined model, so the combined model has enough precision to carry out the electromagnetic loss analysis in the next section.

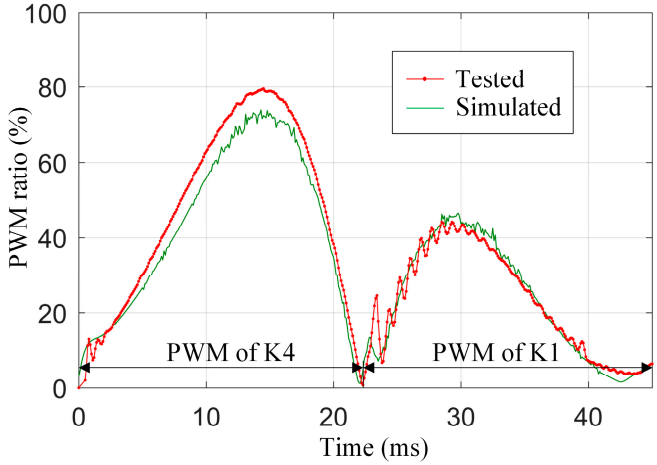

Figure 10. Comparison of the tested and simulated PWM ratio.

4. Electromagnetic Loss Analysis

Based on the validated model in the last section, the electromagnetic loss and power conversion efficiency of the linear motor system designed for the FPEG are simulated and analyzed in this section. Considering that the linear motor system works in generating mode all the time during the stable running of the FPEG, a standard cycle is designed firstly according to the rated operating conditions of the FPEG. As shown in Figure 11, the linear motor system works in generating mode all the time during the standard cycle. The working frequency of the standard cycle is 50 Hz, which is equal to

3000 turns per minute of conventional engines. The coil current amplitude of the linear motor is 22 A, and the reciprocating stroke of the piston-mover movement is 36 mm.

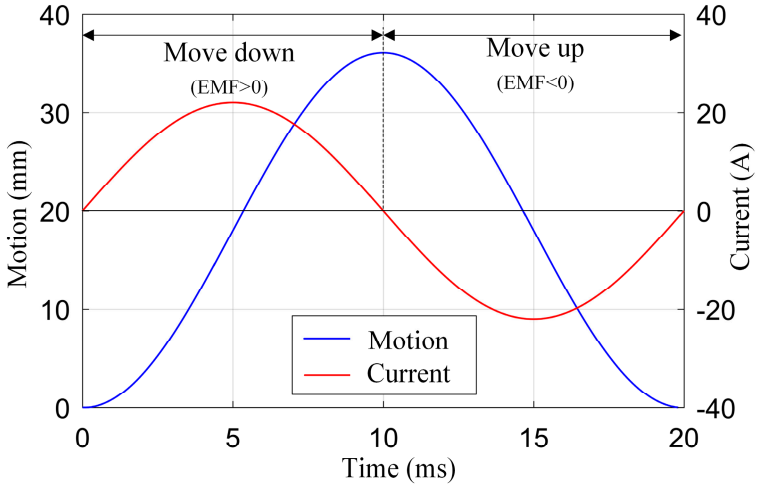

Figure 11. Standard cycle for electromagnetic loss analysis.

Figure 12 shows the simulated instantaneous electromagnetic loss power in the linear motor of the standard cycle. Between the losses, the copper loss of coil accounts for 87% of the total loss. The copper loss depends on the winding wire diameter and is limited by the maximum allowable mass of the moving-coil, thus it is difficult to reduce. The eddy loss of the magnet is small, and this helps prevent the magnet from high temperatures and demagnetization. The eddy loss of the iron core is acceptable. This indicates that the electrical pure iron "DT4" is a suitable choice for the core material and sheets are not necessary. The figure also indicates that the aluminum alloy is not a good choice for the shell material, as the eddy loss is higher than expected.

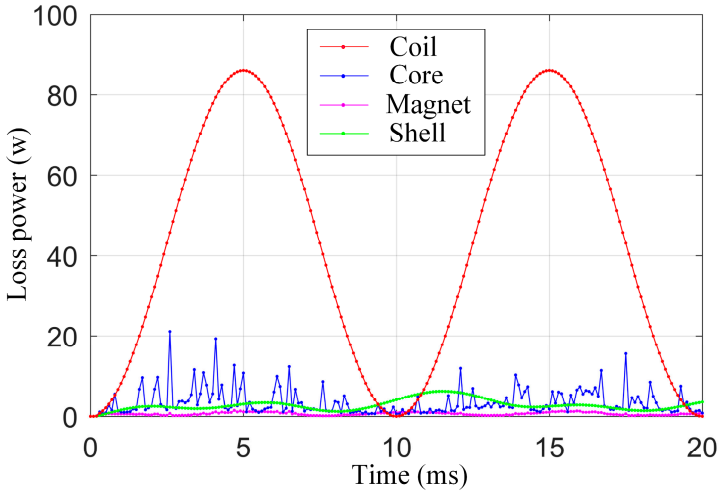

Figure 12. Electromagnetic loss in the linear motor.

Figure 13 shows the simulated instantaneous electromagnetic loss in the rectifier of the standard cycle. It can be seen that the loss power of each MOSFET is different, and it is related to their working states. Take the first half of the cycle to analyze. The EMF and current of the linear motor are positive, so the K3 is controlled by PWM signals and the others remain off. The current flows past the diode of K1 all the time, and its loss is the biggest. When the K3 PWM is off, the current flows past the diode of the K4, and its loss is the second biggest. No current flows past the K2 during the first half of the cycle, so its loss is zero. By analyzing the results, we can conclude that the diodes in the rectifier should be improved, as they account for most of the loss in the PWM rectifier.

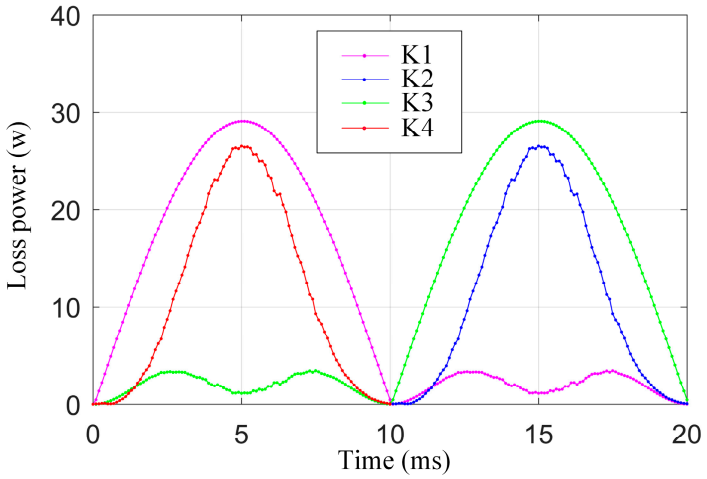

Figure 13. Electromagnetic loss in the PWM rectifier.

Table 3 lists the main parameters and the efficiency of the linear motor system designed by this paper for a FPEG. Under the standard working cycle of rated frequency 50 Hz and rated stroke 36 mm, the generating efficiency of the linear motor and the power conversion efficiency of the rectifier are 91.6% and 94.1%, respectively. The efficiency of the linear motor system is 86.3%. Considering the indicated thermal efficiency of engine is about 37% [17], the efficiency of the chemical-to-electrical energy conversion of about 31% can be obtained by the FPEG system, when it uses the motor system.

Table 3. Parameters and efficiency of the linear motor system.

Name	Value
Rated motion frequency	50 Hz
Rated motion stroke	36 mm
Rated output power	540 W
Mass of the mover	1.2 kg
Efficiency of the linear motor	91.6%
Efficiency of the rectifier	94.1%
Efficiency of the motor system	86.3%
Specific power of the motor	118 W/kg

5. Conclusions

In this paper, a linear motor system composed of a moving-coil linear motor with axial magnetized magnets and an H-bridge PWM rectifier is designed for a portable free-piston engine generator. A combined electromagnetic simulation model is presented and validated by the prototype tested results. The electromagnetic loss of the linear motor system is analyzed by using the validated model. Under the rated working frequency of 50 Hz, the efficiency of 86.3% can be obtained by the proposed linear motor system, which meets the requirement of the design.

The electromagnetic analysis indicates that the copper loss is the main loss of the linear motor, and the diode loss is the main loss of the rectifier. The copper loss and the diode loss account for more than 90% of the total loss. In the future, we will try to improve the performance of the linear motor system by optimizing the moving-coil of the linear motor and using independent diodes to replace the internal diode of the MOSFET. We will test the efficiency of the linear motor system under the 50 Hz rated working cycle after manufacturing a more powerful mechanical drive system.

Author Contributions: Y.H. completed the model analysis and finished the manuscript; Z.X. designed the rectifier and provided the guidance; L.Y. designed the linear motor and completed the test; L.L. revised the manuscript. All authors have read and agreed to the published version of the manuscript.

Funding: This work is supported by the National Natural Science Foundation of China (NO. 51875290, 51975297).

Conflicts of Interest: The authors declare no conflict of interest.

References

1. Jia, B.; Zuo, Z.; Tian, G.; Feng, H.; Roskilly, A.P. Development and validation of a free-piston engine generator numerical model. *Energy Convers. Manag.* **2015**, *91*, 333–341. [CrossRef]
2. Hanipah, M.R.; Mikalsen, R.; Roskilly, A.P. Recent commercial free-piston engine developments for automotive applications. *Appl. Therm. Eng.* **2015**, *75*, 493–503. [CrossRef]
3. Woo, Y.; Lee, Y.J. Free piston engine generator: Technology review and an experimental evaluation with hydrogen fuel. *Int. J. Automot. Technol.* **2014**, *15*, 229–235. [CrossRef]
4. Yang, L.; Xu, Z.; Liu, L.; Liu, N.; Yu, H. A Tubular PM linear generator with a coreless moving-coil for free-piston engines. *IEEE Trans. Energy Convers.* **2019**, *34*, 1309–1316. [CrossRef]
5. Yan, L.; Zhang, L.; Jiao, Z.; Hu, H. Armature reaction field and inductance of coreless moving-coil tubular linear machine. *IEEE Trans. Ind. Electron.* **2014**, *61*, 6956–6965. [CrossRef]
6. Tan, C.; Li, B.; Ge, W. Thermal quantitative analysis and design method of bi-stable permanent magnet actuators Based on multi-physics methodology. *IEEE Trans. Ind. Electron.* **2019**. [CrossRef]
7. Yu, X.; Li, B.; Zhang, T. Variable weight coefficient optimization of gearshift actuator with direct-driving automated transmission. *IEEE Access* **2020**, *8*, 4860–4869. [CrossRef]
8. Wang, J.; West, M.; Howe, D.; Parra, H.; Arshad, W. Design and experimental verification of a linear permanent magnet generator for a free-piston energy converter. *IEEE Trans. Energy Convers.* **2007**, *22*, 299–306. [CrossRef]
9. Xu, Z.; Chang, S. Improved moving coil electric machine for internal combustion linear generator. *IEEE Trans. Energy Convers.* **2010**, *25*, 281–286.
10. Chen, H.; Liang, K.; Nie, R.; Liu, X. Three dimensional electromagnetic analysis of tubular permanent magnet linear launcher. *IEEE Trans. Appl. Supercond.* **2018**, *28*, 1–6. [CrossRef]
11. Zheng, P.; Tong, C.; Bai, J.; Yu, B.; Sui, Y.; Shi, W. Electromagnetic design and control strategy of an axially magnetized permanent-magnet linear alternator for free-piston Stirling engines. *IEEE Trans. Ind. Electron.* **2012**, *48*, 2230–2239. [CrossRef]
12. Xu, Y.; Zhao, D.; Wang, Y.; Ai, M. Electromagnetic characteristics of permanent magnet linear generator (PMLG) applied to free-piston engine (FPE). *IEEE Access* **2019**, *7*, 48013–48023. [CrossRef]
13. Chen, H.; Zhao, S.; Wang, H.; Nie, R. A novel single-phase tubular permanent magnet linear generator. *IEEE Trans. Appl. Supercond.* **2020**, *30*. [CrossRef]
14. Park, M.; Choi, J.; Shin, H.; Lee, K. Electromagnetic analysis and experimental testing of a tubular linear synchronous machine with a double-sided axially magnetized permanent magnet mover and coreless stator windings by using semi-analytical techniques. *IEEE Trans. Magn.* **2014**, *50*, 1–4. [CrossRef]
15. Shin, K.; Jung, K.; Cho, H.; Choi, J. Analytical modeling and experimental verification for electromagnetic analysis of tubular linear synchronous machines with axially magnetized permanent magnets and flux-passing iron poles. *IEEE Trans. Magn.* **2018**, *99*, 1–6. [CrossRef]
16. Yan, H.; Xu, Z.; Lu, J.; Liu, D.; Jiang, X. A reciprocating motion control strategy of single-cylinder free-piston engine generator. *Electronics* **2020**, *9*, 245. [CrossRef]
17. Lu, J.; Xu, Z.; Liu, D.; Liu, L. A Starting control strategy of single-cylinder two-stroke free-piston engine generator. *J. Eng. Gas Turbines Power* **2020**, *142*, 1–11. [CrossRef]